

Site response estimation at Granada city (Southern Spain) based on deep earthquake records



G. Alguacil, F. Vidal

Instituto Andaluz de Geofísica & Dpto. Física Teórica y del Cosmos. University of Granada, Spain.

M. Feriche

Instituto Andaluz de Geofísica. University of Granada, Spain.

SUMMARY:

The city of Granada (Southern Spain) is in an area of moderate seismicity, but suffered in the past damaging earthquakes. It presents the highest hazard in Spain (0.24g for a 475 years return period). On 11 April 2010 a deep (613 km) earthquake of magnitude $M_w=6.3$ occurred with epicentre close to Granada and was recorded on several accelerographs and seismic stations on the city and a nearby station on bedrock. We used the technique of spectral ratio respect the reference station on solid rock to assess the site response at soil sites in Granada city. Significant amplification peaks appear at 1Hz and 1.5-2Hz with values above 7. H/V spectral ratio confirm some of the peaks and suggest multimode vibrations at several stations, perhaps associated to the basin modes. A simulation of a shallower focus similar earthquake show important amplification of PGA and response spectra for the soil sites in Granada.

Keywords: site response, deep earthquake, Granada.

1. INTRODUCTION

Granada city (Southern Spain) is in the zone of maximum seismic hazard in Spain, according to the seismic code NCSE-2002, with expected (rock) acceleration of 0.24g in 475 years. Several works (e.g. Morales et al., 1991; Ibañez et al., 1991, Morales et al., 1993; Kagawa et al., 1996) have shown local amplification effects, due to the shallow geological structure and to the presence of deep sedimentary depocentres forming the Granada Basin. Nevertheless, the occurrence of strong motions in Granada has long return periods and no accelerograms of damaging earthquakes affecting Granada are available up to date. Most studies have been based on small local earthquakes, coda waves, microtremor analysis or macroseismic observations for low-level intensities. Several authors have modelled the seismic response of Granada Basin (Al-Yuncha, 2003; Gil-Cepeda et al., 2002), but only for frequencies under 1Hz, due to the lack of detailed knowledge of the basement topography and the basin structure.

On 11-April-2010 a deep earthquake ($h=613\text{km}$) of $M_w=6.3$ occurred with epicentre close to Granada city. The ground accelerations did not reach 1 gal at any point, but the ground motion was well recorded at several high resolution accelerographs and some broad-band seismograph in the city and at a rock site near it (Fig.1). The wave path is practically vertical and identical for all these stations, except for the shallower structure, which has to be the only responsible of the observed differences between the records. This condition is also fulfilled by teleseismic waves, but they rarely contain enough energy at frequencies of engineering interest to outstand over ground noise in an urban area. Another advantage of this earthquake is that, due to the very deep focus, only locally-generated surface waves are present.

Deep earthquakes have seldom been used for analysis of spectral characteristics of site effects (e.g., Miksat et al., 2008; Sokolov, 2008). The reason is that radiation pattern correction often may be relevant and not always a close rock station is available. In this case, the take-off angles to all the

stations do not differ more than 1 degree, assuring the same path except for the local structure. The reference station is at 10km away from the city on hard rock ($V_{s30} > 1500\text{m/s}$, NEHRP/IBC). This earthquake may yield information not only on the very shallow structure ($< 30\text{m}$), but also on the deposits over the basement, that for some points is as thick as 2800m (Morales et al., 1993; Rodríguez-Fernández & Sanz de Galdeano, 2006).

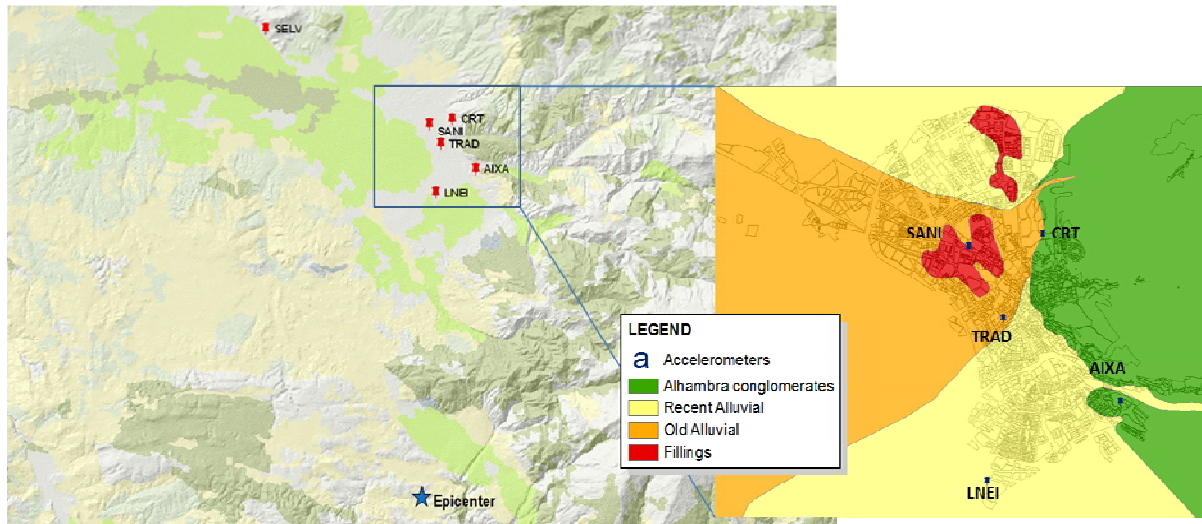


Figure 2.1. Situation of the stations and the deep earthquake epicentre. Left: general view of Granada Basin, the city of Granada the epicentral zone and the reference station SELV. Right: detail of soil stations in Granada city.

2. DATA

We used the records of 7 stations, (six of them operated by the Instituto Andaluz de Geofísica). Six stations are in the city. The other one, SELV, used as reference, is situated at Sierra Elvira in an underground vault at 10km from the city, where a broad-band Streckeissen STS-2 seismometer with high resolution recorder (Earth Data) is installed together with an accelerograph. In this case, the acceleration did not reach the trigger threshold and we used instead the broad-band record. The rest of instruments are 3 Guralp CMG-5TD, 1 Kinematics Etna and 2 Terra Technology IDS. The epicentral distances are between 21 and 32 km (Fig. 2.1). The soil classification for each station is shown in table 2.1. In the stations equipped with IDS, the instruments were triggered twice, for P and S arrivals. **To obtain the corrected traces of velocity and acceleration and compare peak values of homogeneous data,** the row traces were corrected for instrument response, filtered between 0.1-20 Hz, and accelerograms were integrated to velocity (Fig. 2.3). The peak values at each station are listed in table 2.2. For all the stations on soil, these peaks are a factor 2-3 times the ones at the hard rock site SELV.

Table 2.1. Soil types under the stations used. Last column indicates the classification according the Spanish Seismic Code NCSE-02.

Station	Soil type	Class NCSE-02
SELV	Crystalline rock	I
CRT	Conglomerates Alhambra formation-transition	I-II
LNEI	Recent alluvial deposits	II
TRAD	Old alluvial deposits	III
SANI	Alluvial deposits river Beiro	III
AIXA	Conglomerates Alhambra formation	I
FACU	Old alluvial deposits	III

Table 2.2. Peak acceleration values (PGA) and velocity (PGV) at each station and component. The asterisks indicate that PGA was for P wave at that component. PGA is in gal and PGV in cm/s.

Station	PGA E	PGA N	PGA Z	PGV E	PGV N	PGV Z
SELV	0.16	0.12	0.077	0.041	0.027	0.013
CRT	0.31	0.39	0.36 (P)*	0.057	0.065	0.036
FACU	0.34	0.37	0.26	0.061	0.062	0.031
AIXA	0.40	0.40	0.33 (P)*	0.055	0.060	0.046
LNEI	0.35	0.30	0.26	0.053	0.051	0.037
TRAD	0.30	0.34	0.39 (P)*	0.060	0.054	0.037
SANI	0.38	0.44	0.43 (P)*	0.063	0.088	0.035

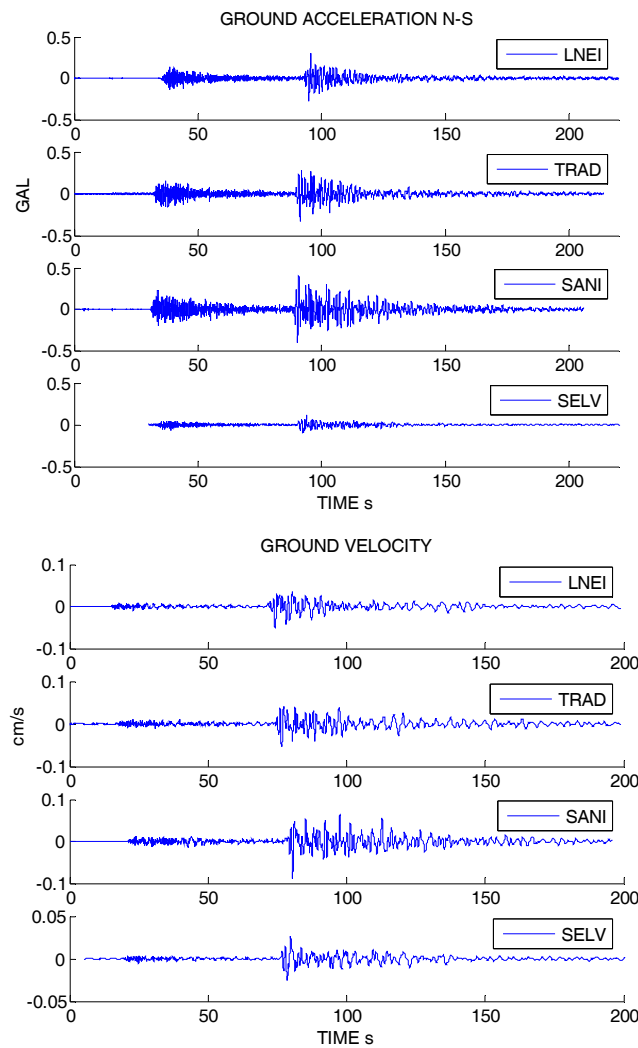


Figure 2.3. Traces of four of the stations used, component N-S. Above: ground acceleration. Below: ground velocity. Note the difference in acceleration amplitude with the reference rock station SELV. Time origin is not the same for all channels.

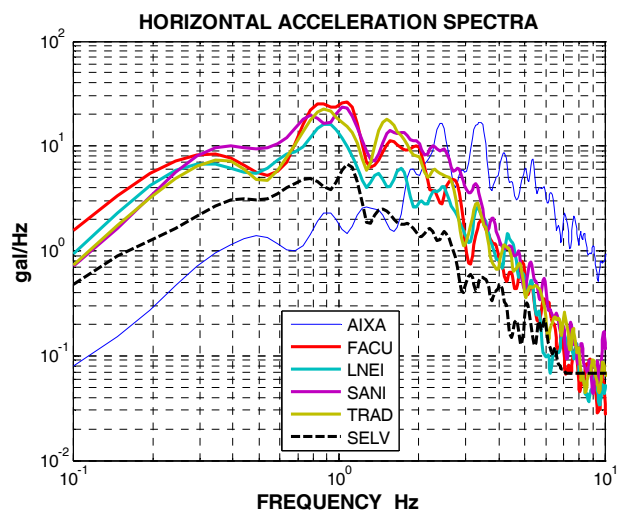


Figure 3. Combined S wave horizontal spectra for the stations used. Solid lines: stations on soil. AIXA spectrum is drawn with a narrow line; it shows severe noise contamination above 2Hz and was not used in the analysis. Dashed line is the spectrum of SELV, used as reference station.

3. ANALYSIS

We selected a 20s window after the S wave arrival, where the most of the S wave train is contained. The smoothed amplitude acceleration spectra of all the traces were calculated (Fig. 3). The acceleration spectrum of station SELV was used as reference and the ratio between the composed horizontal spectra for the other stations and the horizontal combined spectrum of SELV were calculated.

We discarded the spectral ratio for the stations CRT and AIXA, since the IDS records seems not to have enough resolution in this case and the SNR is poor, especially for frequencies above 1-2 Hz. The other spectral ratios show a contamination with the P wave coda above ~10Hz, so we limited the analysis to this frequency (Fig. 4).

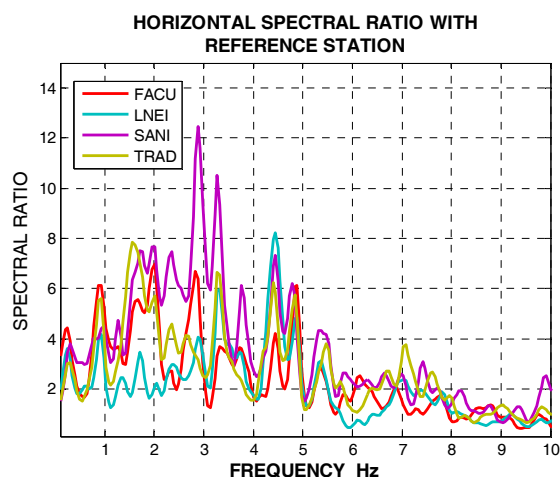


Figure 4. Spectral ratios with the reference station (SELV) for the horizontal S wave spectra at four stations on soil. The stations with less consolidated alluvial soils present the highest peaks.

For each station, the H/V spectral ratio was calculated also using the same S wave window and it is

shown in Fig. 5. Several peaks are coincident with the ones observed in the spectral ratio with the reference station, with quite different amplitudes.

The velocity response spectra were also computed for the horizontal components and combined as the root of the mean square. They are drawn in Fig. 6.

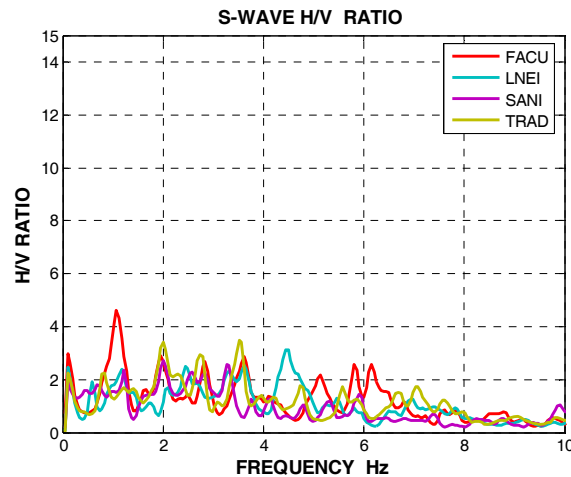


Figure 5. S wave horizontal to vertical spectral ratio for each station. The frequency of some peaks coincide with the peaks of the ratio with the reference station, but the amplitudes are lower. Some of the H/V peaks, like the 2Hz one, appear for all stations, but are not clear in Fig. 4.

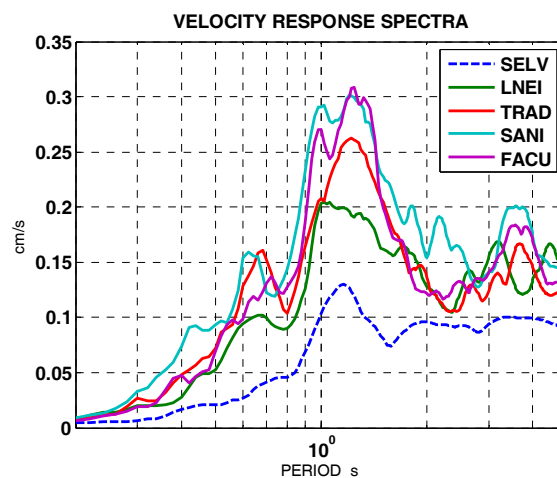


Figure 6. Velocity response spectra (5% damping) for the stations on soil (solid lines) and for the reference station SELV (dash line), on hard rock.

4. A SIMULATION EXAMPLE

Ground motion is the result of contributions of the source radiation, the wave propagation between the source and the station basement and the local site response. In this case, the transfer function accounting for the wave propagation common to all the stations used is approximately known and this permit the estimation of the expected ground motion at every site for a similar earthquake with focus at a shallower depth. This is not unrealistic, since that kind of events have occurred in the past (e.g. in 1884 an earthquake of estimated magnitude 6.5-6.7 caused severe damage in the zone; in 1432 a destructive seism affected heavily Granada city), although most recent activity –last century- did not exceed magnitude 5 in this area. We chose to simulate the S wave train for an earthquake with the same source and site effects, but at a depth of 15km, since most of seismicity in the Granada Basin

area occurs above this depth (Morales et al, 1997).

Far-field displacement spectrum of S wave $D(f)$ may be modelled (e.g., Brune, 1970, Hanks & Wyss, 1972) except for the site effect, with a Brune source, a geometrical spreading factor for body waves and an attenuation operator $A(f)$ dependent of frequency. If f_0 is the corner frequency of the source, M_0 its scalar moment, ρ and β the density and shear-wave velocity in the source region, $\Psi_{\theta\phi}$ the source radiation pattern and K a factor accounting for the free surface and the transmission coefficients of the different discontinuities that the wave cross in its path,

$$D(f) = A(f) \cdot \Psi_{\theta\phi} \cdot \frac{K \cdot M_0}{1 + \frac{f^2}{f_0^2}} \frac{1}{4\pi\rho\beta^3} \frac{1}{R} \quad (1)$$

Where the attenuation factor is

$$A(f) = \exp\left(-\frac{\pi f t}{Q_0 \cdot f^\eta}\right) \quad (2)$$

Here t is the wave travel time, Q_0 is the effective (average) quality factor of the path at frequency $f=1\text{Hz}$ and η accounts for the frequency dependence of the quality factor.

With these expressions, we may simulate a realistic accelerogram for the same source at a shallower depth, thus less attenuated by the geometrical spreading and the anelasticity (eq. 2). Effective (average) attenuation factor $A(f)$ in this case is almost completely due to the mantle path and was estimated using the known source parameters by a manual fit of $D_1(f)$ to the observed S spectrum on SELV (rock). We used $Q_0=120$ and $\eta=0.6$, in accordance with the obtained recently by Mancilla et al. (2012) from records of this same earthquake. Then we calculated $D_2(f)$ for a crustal path, using the values of $A(f)$ found by Ibáñez et al., (1991). Then the factor $D_2(f)/D_1(f)$ was applied to the observed spectrum at each site and its inverse transform yielded the time simulation. We selected the new hypocentral distance for $D_2(f)$ such that the accelerogram “on rock” has amplitude of approximately 0.1g. Our objective is to use the observed frequency-dependent factors (fig. 4) to scale accordingly this accelerogram for the soil sites. The results of this simulation are shown in Fig. 7 and 8.

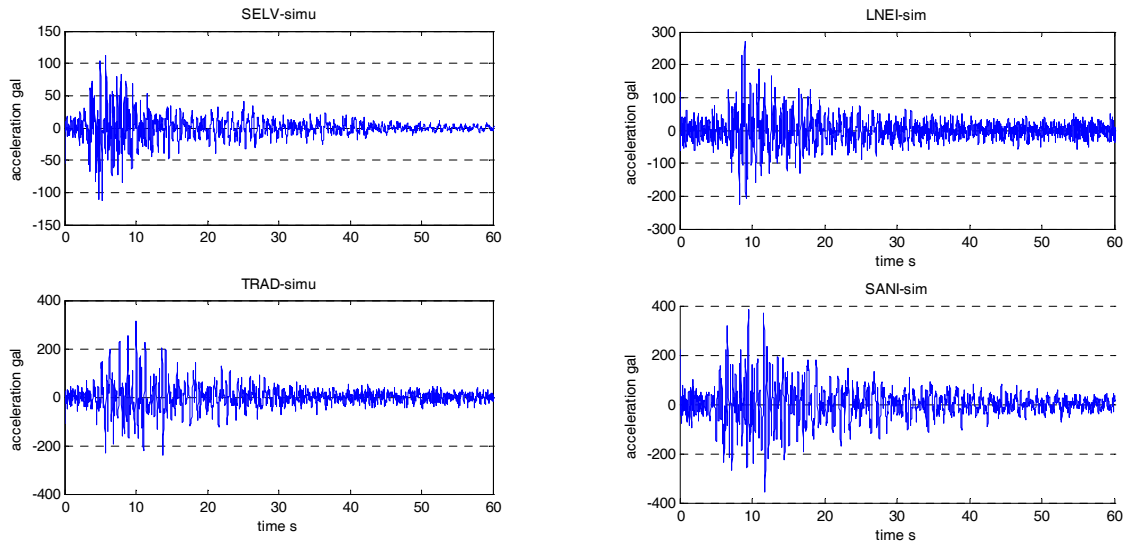


Figure 7. Simulated accelerograms for S wave obtained by scaling the real ones with a frequency-dependent factor to account for the anelastic attenuation. Upper left is the accelerogram obtained at the rock station SELV. The others are calculated for the soil sites. Note the different scales of y-axes. As expected, the maximal PGA is for the station SANI, on alluvial soil.

The simulations for the soil sites result noisier than the one for SELV (rock), due to the fact that the original real accelerograms itself contain noise, since they were obtained in an urban area and the

ground motion had low amplitude. Furthermore, the scaling factor increases with frequency, amplifying the high-frequency noise. The acceleration response spectra for these simulations are shown in Fig. 8, together with the design spectra of the Spanish seismic code (NCSE-02) for each type of soil, for reference. The SA for SELV is under the limits for periods under 1s, since we have scaled to a PGA ($\sim 0.1g$) less than half the prescription PGA ($0.24g$). In the soil cases, the spectra of the code are not higher, but wider. The simulated ones are clearly above it for a wide range of periods.

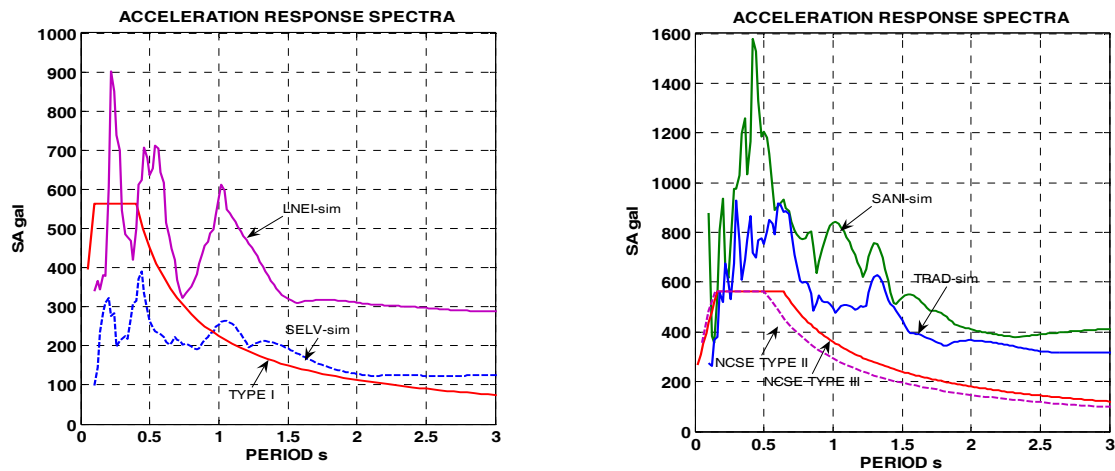


Figure 8. Acceleration response spectra for the simulated accelerograms. Left, dashed line, the reference simulation on rock (SELV) and the one for the hardest soil (LNEI). Right, the two simulations for the sites on soils types II (TRAD) and III (SANI). The reference SA of the Spanish code for each soil type are also drawn.

5. DISCUSSION

The accelerograms analysed contain enough energy at engineering frequencies to stand out above urban noise. The stations share a common wave path except for the local structure under each one. So the spectral ratio respect a reference rock station (SELV) shows the main features of each site effects. The analysis was limited to the band 0.1-10Hz, where the P coda contamination was not relevant. Two stations were discarded in this analysis because its low resolution.

Significant peaks of spectral ratios are present at 1Hz and 1.5-2Hz., with values above 7 for the softest soils. Some other peaks appear at all stations, but these should be carefully interpreted, since the reference station spectrum (denominator) presents valley at the same frequencies.

H/V ratios reproduce several of these peaks, with different level, and show other coincident peaks at several stations. Given the different site conditions, these latter peaks are more likely explained by deeper layers common to them or by excited basin modes, though this requires further investigation.

The response spectra show maxima for periods of 0.4-0.5s and, most prominent, for 1.0-1.4s, with amplitudes about 3 times the reference station on rock.

The simulation of accelerograms with higher level and high-frequency enhanced, to account for a hypothetical shallower focus, where most of seismicity of the zone occurs, show realistic ground motions with the same spectral ratios to the reference station, thus preserving the site response. The peak ground acceleration is more than a factor 3 the one on rock for the alluvial softest soil and more than double for the other soil sites. The response spectra show in this case a low period maximal for LNEI –a station on hard soil-, with relevant peaks at 0.5 and 1s. The softest site (SANI) present a high peak at 0.5s and also at 1s.

6. CONCLUSIONS

The common wave path to several stations, except for the different site conditions, in Granada city urban area and a nearby solid rock station, together with the signal energy content in the engineering frequency band (~0.2-10Hz) made the records of the M_w 6.3 deep earthquake of 11-4-2010 provide valuable information to assess the site effects at several points of the city, affected in the past by destructive earthquakes. The spectral ratio of S between wave packet of the stations on soil and the reference station on rock show spectral amplification at frequencies 1Hz, 1.5-2Hz (up to a level of 7 times) and for 3Hz and higher frequencies for some stations. The H/V spectral ratio confirms several of these peaks and seems to show multimode vibrations, especially for some stations.

A realistic simulation of an earthquake with the same source and shallower focus shows the relative amplifications also for higher frequencies and peak acceleration above 3 times the one on rock for some soil sites. The response spectra show peaks at 0.25s for the hard soil site and at 0.5 and 1s for some others; at the softest soil, a peak at 1s is about 4 times the peak response at rock.

ACKNOWLEDGEMENT

This work was carried out as part of the research project: CGL2007-66745-C02-01-02/BTE, funded by the Spanish Ministry of Science and Innovation. The record of station FACU was kindly provided by Prof. López-Casado.

REFERENCES

- Al-Yuncha, Z. (2003): “Evaluación de las características principales del movimiento sísmico en un lugar específico usando técnicas numéricas de modelado”. Tesis doctoral. Universidad de Granada.
- Brune, J.N. (1970): Tectonic stress and spectra of seismic shear waves. *Journal of Geophysical Research*, **75**, 4997-5009.
- Gil-Zepeda, A., Luzón, F., Aguirre, J., Morales, J., Sánchez-Sesma, F. y Ortiz-Alemán, C. (2002): “3D Seismic Response of the Deep Basement Structure of the Granada Basin (Southern Spain)”. *Bull. Seism. Soc. Am.* **92**, 2163-2176.
- Hanks, T.C. & Wyss, M. (1972): The use of body-wave spectra in the determination of seismic-source parameters. *Bull. Seism. Soc. Am.*, **72:2**, 561-589.
- Ibáñez, J.M., Morales, J., De Miguel, F., Vidal, F., Alguacil, G. y Posadas, A.M. (1991): “Effect of a sedimentary basin on estimation of Q_c and Q_{lg} ”. *Physics of the Earth and Planetary Interiors*, **66**, 244-252.
- Kagawa, T. and Group for Spanish-Japanese Joint Work on Microzonation of Granada Basin (1996), “Microtremor Array Observation in the Granada Basin, Southern Spain”. In *Homenaje en honor al profesor Fernando de Miguel Martínez*, 287-304. Universidad de Granada.
- Miksat, J.; K.-L. Wen, Ch.-T. Chen., V. Sokolov and F. Wenzel (2008): “Exploring Site Response in the Taipei Basin with 2D and 3D Numerical Simulations”. Proc. of the *14th World Conf. on Earthquake Engineering*. October 12-17, 2008, Beijing, China
- Mancilla, F., Del Pezzo, E., Stich, D., Morales, J., Ibáñez, J. and Bianco, F. (2012) “QP and QS in the upper mantle beneath the Iberian peninsula from recordings of the very deep Granada earthquake of April 11, 2010”. *Geophysical Research Letters*, **39**, L09303, doi:10.1029/2012GL050947.
- Morales, J., Ibáñez, J.M., Vidal, F., De Miguel, F., Alguacil, G. y Posadas, A.M. (1991): “ Q_c site dependence in the Granada Basin (Southern Spain)”. *Bull. Seism. Soc. Am.* **81**, 2486-2492.
- Morales, J., Seo, K., Samano, T., Peña, J.A., Ibáñez, J.M. y Vidal, F. (1993): “Site response on seismic motion in the Granada Basin (Southern Spain) based on microtremor measurements”. *J. Phys. Earth*, **41**, 221-238.
- NCSE-02 (2002): “Normativa de Construcción Sismorresistente Española. Comisión Permanente de Normas Sismorresistentes”, *Real Decreto 997/2002. Boletín Oficial del Estado No. 244*, 11 October, 2002, Spain.
- NEHRP (2003), “Recommendation provision for seismic regulation for new buildings and other structures”, *Building Seismic Safety Council*, Washington, D. C Federal Emergency. FEMA.
- Rodríguez-Fernández, J. y Sanz de Galdeano, C. (2006): Late orogenic intramontane basin development: the Granada basin, Betics (southern Spain). *Basin Research* **18**, 85–102,
- Singh, S.K., Apsel, R.J., Fried, J. and Brune, J.N. (1982). Spectral attenuation of SH-waves along the Imperial fault. *Bull. Seism. Soc. Am.*, **72**, 2003-2016.
- Sokolov, V., Wen, K.-L., Miksat, J., Wenzel, F., Chen C.-T. (2008): “Analysis of Taipei basin response on earthquakes of various depth and location using empirical data”. 31st General Assembly of the European Seismological Commission ESC 2008, Hersonissos, Crete, Greece.